Korean J. Chem. Eng., 38(5), 1014-1022 (2021)
DOI: 10.1007/s11814-021-0765-9

pISSN: 0256-1115
eISSN: 1975-7220

Enhancing the separation and antifouling properties of PES nanofiltration membrane by use of chitosan functionalized magnetic nanoparticles

Farhad Zareei, Samaneh Bandehali, and Sayed Mohsen Hosseini†

Department of Chemical Engineering, Faculty of Engineering, Arak University, Arak 38156-8-8349, Iran
(*Received 1 September 2020 • Revised 7 February 2021 • Accepted 23 February 2021*)

Abstract−Chitosan functionalized ($CoFe_2O_4$-CuO) composite nanoparticles were synthesized and then used in fabrication of PES-based nanofiltration membranes. X-ray diffraction, Fourier transform infrared spectroscopy and scanning electron microscopy were used for the characterization of synthesized nanoparticles. The fabricated membranes were also characterized by scanning electron microscopy, 3D surface images, water contact angle, membrane porosity, pure water flux, salt rejection and fouling resistance consideration. Obtained results revealed that water contact angle was reduced significantly from 65° for the neat membrane to 36° for M5 with 1.0 wt% composite nanoparticles. All modified membranes also showed higher water flux and salt rejection than virgin PES membrane. The highest pure water flux measured 45.2 L/m^{2}h and the highest salt rejection measured 88% for the modified membranes containing of composite nanoparticles. The modified membranes showed outstanding antifouling ability. The flux recovery ratio enhanced from 40% for pristine membrane to 93% for the modified ones with 0.5 wt% of Cs-functionalized ($CoFe_2O_4$/CuO) composite nanoparticles.

Keywords: Nanofiltration, Mixed Matrix Membrane, Chitosan-functionalized [$CoFe_2O_4$/CuO] Nanoparticles, Synergetic Effect, Separation/Antifouling Property

INTRODUCTION

Nanofiltration (NF) membranes are applied widely for water treatment due to their compact design, simplicity of operation, low consumption of energy and lack of phase change [1]. High separation efficiency is another major reason for broad application of NF-membrane [2,3]. However, producing NF membranes with special adapted characteristics such as high flux and rejection, good mechanical and chemical stability as well as suitable antifouling activity is a vital step in future membrane-based wastewater treatment application. The fouling phenomenon occurs as the result of undesirable adsorption and the foulant sedimentation on the surface or into the pores of membrane that leads to decrease of flux [4]. The physico-chemical characteristics of membrane, such as hydrophilicity and roughness, as well as the nature of the feed solution and operating conditions, are important parameters that affect membrane fouling [5]. Various strategies, such as the choice of a suitable material for membrane construction [6], pretreatment of feed [7], optimization of the operating conditions [8] and the backwashing and back-pulsing methods [9] have been used to reduce the fouling phenomenon. Notably, the earlier reported studies reveal that tailoring the surface characteristics of NF-membranes, such as improvement of surface hydrophilicity and decrease of surface roughness, can promote the antifouling activity of them since most of the foulants are in nature hydrophobic [10]. For the purpose, several approaches have been adopted to producing highly efficient NF membranes including photo-grafting of hydrophilic monomers, chemical modification, plasma treatment, as well as the employment of various filler additives such as nanomaterials [11-15]. Introducing nanoparticles as one of the most desirable, helpful and effective method has attracted much attention [16,17]. Application of inorganic nanomaterials into the polymeric membranes has been examined in numerous applications to improve their physico-chemical and separation properties, antifouling ability and stability due to the synergistic effect resulting from combining of components [13,18-21]. Meanwhile, composite metal oxides such as spinal ferrites are favorable nanoparticles that have been widely implemented in water purification during the last decades. Cobalt ferrite ($CoFe_2O_4$) as a magnetic nanoparticle with excellent adsorption properties, high surface area and chemical stability was investigated in a wide range of applications from drug delivery to water treatment. Also, the earlier researches proposed effective procedures to producing outstanding magnetic based nanomaterials by the combination of other nanomaterials and ferrites ones. Zangeneh et al. [22] prepared nanocomposite PES-based NF membranes by incorporation of [boron doped-TiO_2-SiO_2/$CoFe_2O_4$] nano photocatalyst. The highest flux and flux recovery ratio was observed by introducing 0.5 wt% of (B-TiO_2-SiO_2/$CoFe_2O_4$) nanoparticles. In another study, Zhang et al. [23] constructed [activated carbon/$CuFe_2O_4$] composite nanoparticles for catalytic regeneration and removal of Acid orange. Also, prepared ($MnFe_2O_4$/activated carbon) nanoparticles were used for tetracycline removal from water [24].

Preparing a novel mixed matrix PES-[chitosan functionalized-($CoFe_2O_4$/CuO) composite nanoparticles] membrane with enhanced separation and antifouling characteristics for the application in nanofiltration process related to wastewater treatment was the primary target of the current study. No research was found in the literature survey for fabrication of polyethersulfone-based mixed matrix

†To whom correspondence should be addressed.
E-mail: s-hosseini@araku.ac.ir
Copyright by The Korean Institute of Chemical Engineers.

nanofiltration membrane by incorporating [chitosan functionalized-($CoFe_2O_4$/CuO)] composite nanoparticles, and the literature is silent on separation characteristic and antifouling ability of (PES/Cs-($CoFe_2O_4$/CuO)) nanocomposite membrane.

Chitosan is a bio-compatible, low toxic and hydrophilic polymer with abundant amino and hydroxyl groups that has been used widely in membrane fabrication, coating materials as well as adsorbents due to its high ability for adsorption of different types of macromolecules, salts and dyes [25-27]. Many studies reported application of chitosan containing membranes for contaminant removal from water by adsorption mechanism [28-30]. Several studies also have considered the construction and modification of nanoparticles by chitosan for the application in polymeric membranes with the aim of promoting separation performance and anti-fouling ability in pollutant removal from aqueous solutions [31-34].

In the current study, mixed matrix (Cs-($CoFe_2O_4$/CuO)) nanofiltration membrane was fabricated by solution casting method through phase inversion technique. The effect of (Cs-($CoFe_2O_4$/CuO)) composite nanoparticle content ratio in the membrane matrix on physico-chemical properties, separation characteristics and antifouling activity of them was studied. The composite nanoparticles were synthesized by chemical precipitation technique and characterized by FTIR, XRD and FESEM. The SEM, 3D surface image, water contact angle, membrane mean pore size and porosity, water flux, salt rejection and antifouling activity measurements were carried out in membranes characterization.

EXPERIMENTAL

1. Materials

Polyethersulfone (PES) supplied from BASF New Jersey, USA (Ultrason E6020P, Mw: 58,000). N, N-Dimethylacetamide (DMAC, Mw: 87.12, 0.94 g/cm^3) and polyvinylpyrrolidone (PVP, 25,000 g/mol) from Merck Inc., Germany, were used as solvent and pore former. $Co(NO_3)_2{\cdot}6H_2O$, $Fe(NO_3)_3{\cdot}9H_2O$, $Cu(NO_3)_2{\cdot}3H_2O$ and NaOH were supplied from Merck Inc., Germany. Acetic acid and glutaraldehyde were also purchased from Sigma Aldrich Company, USA. Chitosan (CS, 100,000-300,000 g/mol, 90% deacetylated, ACROS Inc., USA) was also used. All other chemicals were supplied by Merck, Inc., Germany. Distilled water was used during the experiment.

2. Synthesis of Cs-($CoFe_2O_4$/CuO) Composite Nanoparticles

The $CoFe_2O_4$ nanoparticles were synthesized by chemical precipitation technique. Briefly, $Fe(NO_3)_3{\cdot}9H_2O$ and $Co(NO_3)_2{\cdot}6H_2O$ with stoichiometric ratio of 1 : 2 (Co : Fe) were dissolved in deionized water with for 2 h at 60 °C. Afterwards, NaOH aqueous solution was added to the mixture drop by drop to keep the pH of solution more than 10. Then, the solution was centrifuged and washed with distillate water and ethanol. The precipitate particles were dried for 8 h at 90 °C. Finally, the obtained particles were placed in a furnace at 600 °C for 3 h. For the preparation of ($CoFe_2O_4$/CuO) nanoparticles, 0.33 g of $CoFe_2O_4$ nanoparticles were first dispersed in distilled water. Then 0.15 g of $Cu(NO_3)_2{\cdot}3H_2O$ and 2.5 ml of NaOH (1 M) were added to the mentioned solution. The prepared solution was then sonicated for 1 h. The obtained particles were centrifuged and washed with deionized water and were placed in a furnace at 500 °C for 2 h. For preparation of chitosan functionalized ($CoFe_2O_4$/CuO) composite nanoparticles, 0.5 g of chitosan was dissolved in 50 ml of distilled water containing of 5 wt% acetic acid. The solution was stirred for 15 minutes by a mechanical stirrer. Then 0.35 g of ($CoFe_2O_4$/CuO) nanoparticles was added to the solution and sonicated for 30 min by an ultrasonic bath (Parsonic 11S model, Iran). After that, 50 ml of 1 M NaOH was added to it and stirred for 20 minutes. The solution was sonicated again at 60 °C for 30 min. Finally, 2 ml of glutaraldehyde was added to the solution and sonicated another 2 h at 60 °C. The resulting particles were washed with acetone and deionized water and placed in an oven for 12 h at 50 °C.

3. Preparation of Mixed Matrix NF-Membranes

The PES/Cs-[$CoFe_2O_4$/CuO] NF membranes were fabricated by phase inversion method. For the purpose, PES (18 wt%) and PVP (1 wt%) were dissolved in N, N-dimethylacetamide in a glass reactor equipped with a mechanical stirrer for more than 4 h to obtain a homogenous solution. This was followed by mixing a various amount of synthesized composite nanoparticles into the polymeric solution. The solution was then sonicated for 1 h by an ultrasonic bath (Parsonic 11S model, Iran) to reach a better dispersion of nanoparticles. The resulting solution was left for 24 h at room temperature to remove air bubbles. Then polymeric solution was cast on clean glass plates using a film applicator with 150 μm thickness at ambient temperature. The prepared films were immediately dipped into DI water. Finally, membranes were stored in deionized water for another one day. The composition of casting solution is given in Table 1.

4. Characterization of Synthesized Composite Nanoparticles

The structure of synthesized Cs-($CoFe_2O_4$/CuO) composite nanoparticles was characterized using X-ray diffractometer instrument (model X′ Pert Pw 3373, λ_{Cr}=2.289 °A, Philips, Holland). The average grain size was obtained by Debye-Scherrer equation [35].

$$D = \frac{K\lambda}{\beta\cos\theta} \quad (1)$$

Table 1. The composition of casting solution used in membrane fabrication

Membrane	PES (wt%)	PVP (wt%)	DMAC (wt%)	Cs-[$CoFe_2O_4$/CuO] (wt%)
M (1)	18.00	1.00	81.00	0.00
M (2)	18.00	1.00	80.95	0.05
M (3)	18.00	1.00	80.90	0.10
M (4)	18.00	1.00	80.50	0.50
M (5)	18.00	1.00	80.00	1.00

where K is the equation constant (0.95), λ and β are wavelength of X-ray and the diffraction peak width at its half maximum intensity (FWHM), and θ is the diffraction angle (radian).

Fourier transform infrared (FTIR) transmission spectra (Galaxy series 5000, KBr disc) and scanning electron microscopy (SEM, SU3500, USA) were also used for characterization of composite nanoparticles.

5. Membrane Characterization

5-1. SEM and AFM Analysis

SEM analysis was used to investigate the membrane morphology. For investigation of the surface morphology of membranes, 3D surface images were employed using an optical microscope and SPM software (v 6.4, Femtoscan) in the area of 10 μm×10 μm.

5-2. Measurement of Water Contact Angle, Porosity and Mean Pore Size

The surface hydrophilicity of prepared membranes was determined by using a contact angle analyzer (G10, Kruss, Germany) and distilled water as probe liquid. Five locations of each sample were considered to obtain the contact angle for minimizing experimental errors. After that, the average of measurements was reported.

The overall porosity (ε) of prepared membranes was also obtained by Eq. (2) [36-38]:

$$\varepsilon(\%)=\frac{(w_w-w_d)}{A\times l\times \rho_f}\times 100 \tag{2}$$

where W_w, W_d, L, A, and ρ_f are the weight of wet membrane (g), weight of dry membrane (g), membrane thickness (cm), membrane surface area (cm^2), and water density (g/cm^3), respectively. To minimize experimental error, experiments were carried out three times for each sample and then their average value was reported.

5-3. Filtration Performance of Membranes

A homemade dead-end filtration system with effective area of 11.94 cm^2 was applied to measure the water flux and salt rejection of fabricated membranes (See Fig. 1).

The membranes were initially pressurized with deionized water for 20 min at 6 bar to achieve a steady pure water flux prior to filtration test. Flux of membrane was examined by Eq. (3) [37,38]:

$$J_{w,1}=Q/A(\Delta t) \tag{3}$$

where A denotes the membrane surface area (m^2), Q is the volume of collected permeate (L), $J_{w,1}$ shows the water flux ($L/m^2\cdot h$), and Δt is the filtration time (h).

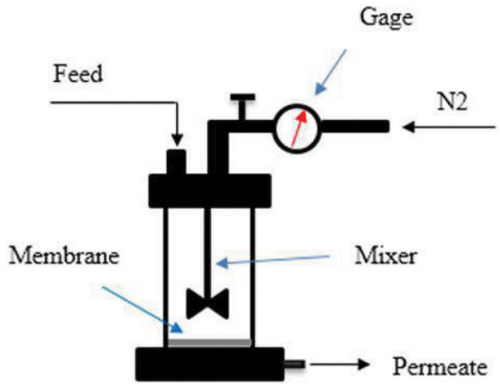

Fig. 1. Schematic diagram of used dead-end filtration cell in this study.

For evaluation of the membrane salt rejection, 0.01 M Na_2SO_4 and NaCl aqueous solutions were used at 5 bar. The following equation was employed for salt rejection evaluation [37]:

$$R(\%)=\left(\frac{C_f-C_p}{C_f}\right)\times 100 \tag{4}$$

where C_p and C_f denote the concentration of salt in permeate and feed, respectively.

5-4. Antifouling Property of Membranes

The powder milk solution was applied as foulant to assess the anti-fouling performance of the prepared membranes. The occurrence of fouling in membrane filtration is the result of protein adsorption into the membrane pores or on the membrane surface. For the membrane fouling studies, after one hour conducting the pure water flux test ($J_{w,1}$, L/m^2h), a 8,000 mg/l of milk powder solution was immediately entered into the cell and the flux across the membrane was measured again at 5 bar for 60 min (J_p, L/m^2h). Fouled membranes were then washed and kept in distilled water for 1 h. The PWF was measured for the washed membranes ($J_{w,2}$, L/m^2h) again. The membrane flux recovery ratios (FRR%) were obtained by Eq. (5) as follows [39,40]:

$$FRR(\%)=\left(\frac{J_{w,2}}{J_{w,1}}\right)\times 100 \tag{5}$$

The fouling in membranes was investigated by hydraulically reversible fouling, which is related to weak attachment of foulants with membrane surface and leads to concentration polarization and irreversible fouling, which is related to tight attachment of foulants with membrane; that leads to adsorption of foulant on the membrane surface due to stable connection. Irreversible fouling leads to increase of operating costs and reduced filtration performance and decrease of lifetime of membrane. Eqs. (6) to (8) were used to obtain three fouling parameters, including R_r, R_{ir} and R_t as reversible fouling ratio, irreversible fouling ratio and total fouling [40]:

$$R_r(\%)=\left(\frac{J_{w,2}-J_p}{J_{w,1}}\right)\times 100 \tag{6}$$

$$R_{ir}(\%)=\left(\frac{J_{w,1}-J_{w,2}}{J_{w,1}}\right)\times 100 \tag{7}$$

$$R_t(\%)=\left(1-\frac{J_p}{J_{w,1}}\right)\times 100 \tag{8}$$

RESULTS AND DISCUSSION

1. Synthesized Nanoparticle Characterization

The X-ray pattern of synthesized Cs-($CoFe_2O_4$/CuO) nanoparticles is shown in Fig. 2. All diffraction peaks are very close to a cubic phase for $CoFe_2O_4$ and CuO with space group Fd3m and Fm3m, respectively. The average grain size was calculated >33 nm. The XRD pattern also exhibited cubic phase for the synthesized Cs-($CoFe_2O_4$/CuO) nanoparticles.

The FT-IR spectrum of synthesized Cs-($CoFe_2O_4$/CuO) nanoparticles is given in Fig. 3. The FT-IR spectrum of nanoparticles dis-

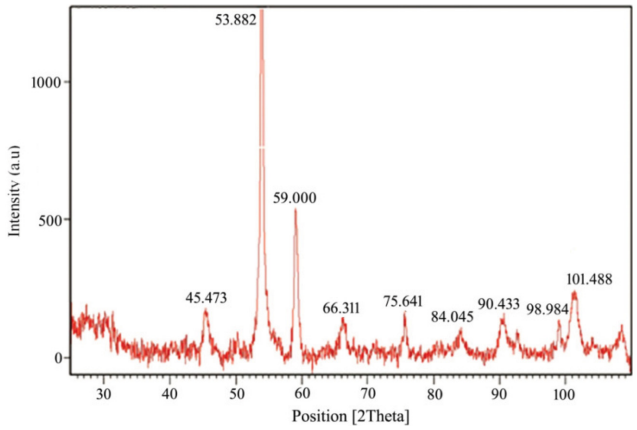

Fig. 2. XRD pattern of synthesized Cs-($CoFe_2O_4$/CuO) nanoparticles.

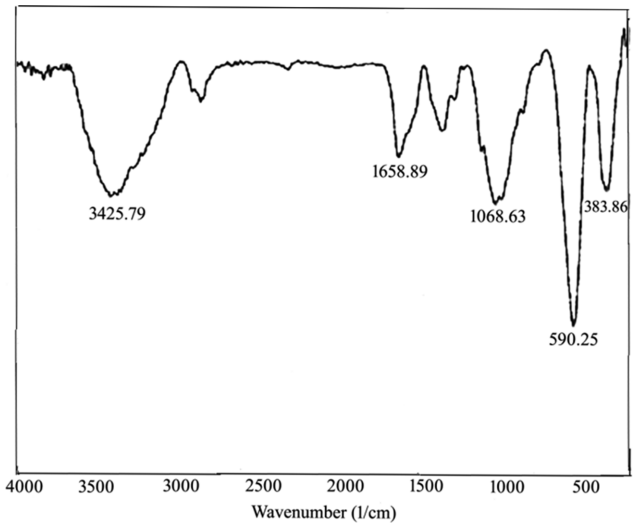

Fig. 3. FT-IR spectrum of synthesized Cs-($CoFe_2O_4$/CuO) nanoparticles.

tinctly displays an absorption peak at 1,068.63 cm^{-1} that is related to the stretching vibration of C-O-C functional groups. A broad peak appears between 3,000-3,700 cm^{-1} which is assigned to N-H and O-H groups of chitosan. Also, an observed peak at 1,658.89 cm^{-1} corresponds to the formation of C=N groups. Two strong absorption bands at 590.25 and 383.86 are also relevant to phonon absorption of $CoFe_2O_4$/CuO lattice [40,41].

Synthesized composite nanoparticles were characterized by SEM. Fig. 4 shows the SEM image of synthesized Cs-($CoFe_2O_4$/CuO) nanoparticles. Images show relatively uniform particle size distribution for the synthesized nanoparticles.

2. Membrane Characterization

2-1. Membrane Morphology

Fig. 5 shows the cross-sectional SEM images of the fabricated membranes. All membranes show an asymmetric structure with finger-like channels. Utilizing of nanoparticles into the membrane matrix changed the membrane morphology by affecting the kinetics and thermodynamics of the phase inversion process. The hydrophilic nature of used nanoparticles enhances the exchange rate between solvent and nonsolvent during the phase inversion, which led to more porosity and formation of more macro-voids for the blended membranes compared to pristine membrane [40-42]. Also, as seen in the images, increase of nanoparticles ratio in the membrane matrix decreased the thickness of top-layer significantly. Formation of a dense skin-layer along with thicker sub-layer and lower porosity for M5 at 1.0 wt% composite nanoparticles may be assigned to increase of the viscosity of polymeric solution at high additive concentration that decreases the solvent-nonsolvent exchange rate [42,43].

Fig. 6 illustrates the SEM surface images for all prepared membranes. Images show the change of surface morphology in modi-

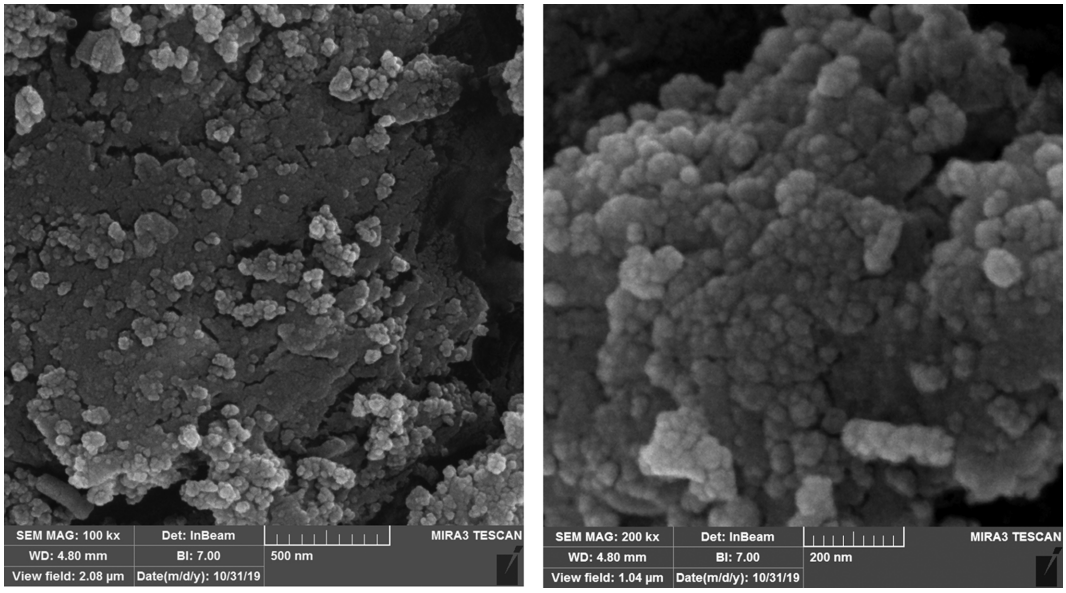

Fig. 4. SEM images of synthesized Cs-($CoFe_2O_4$/CuO) nanoparticles.

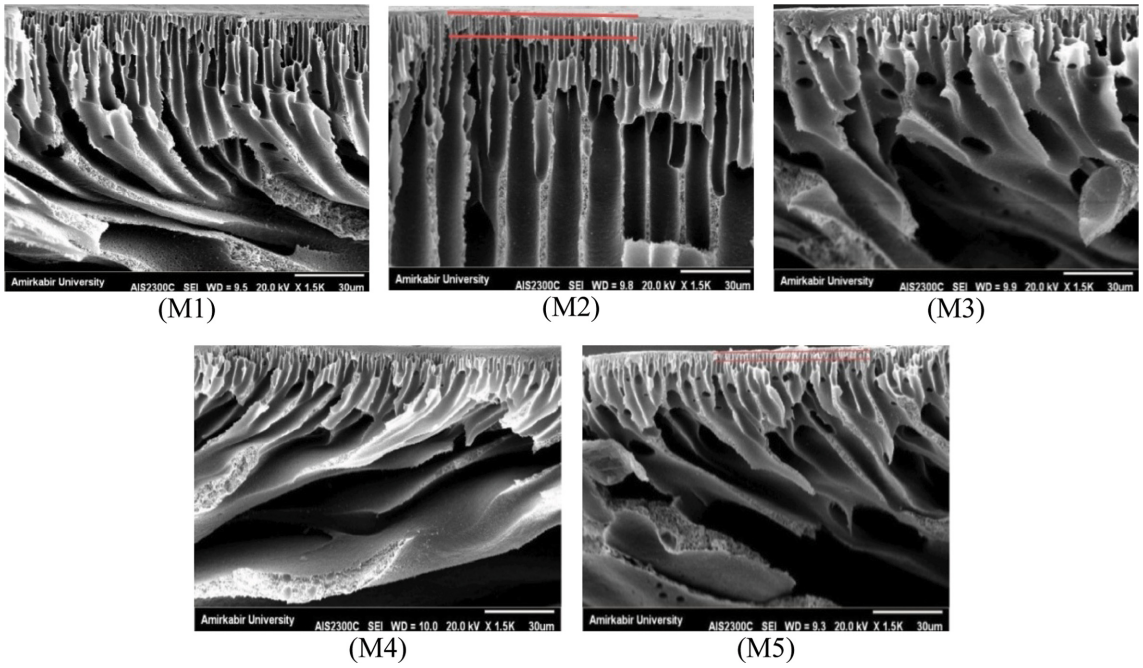

Fig. 5. The cross-section SEM images of fabricated membranes with different concentration of synthesized Cs-($CoFe_2O_4$/CuO) composite nanoparticles.

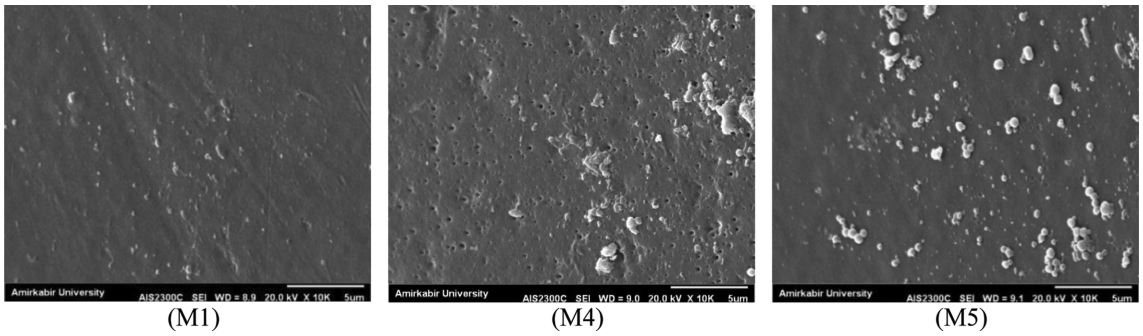

Fig. 6. SEM surface images of fabricated membranes.

fied membranes compared to neat PES-membrane. A relatively uniform surface was observed for the prepared membranes. Some agglomeration of nanoparticles for M5 at high additive concentration is due to tendency of nanoparticles for accumulation naturally [44-46].

Energy dispersive x-ray (EDX) spectroscopy analysis was also used to investigate the nanoparticle dispersion in the membrane matrix. As shown in Fig. 7, the bright spots correspond to Co of nanoparticles that reveal good dispersion for them relatively.

The surface roughness of prepared membranes was investigated by 3D surface images (Fig. 8). Dark areas are related to valleys and the bright ones assigned to the peaks. Results show that incorporation of nanoparticles into membrane matrix clearly led to decrease of surface roughness. The average roughness (Ra) was decreased by embedding composite nanoparticles up to 0.5 wt% in the membrane matrix. The relative uniform dispersion of nanoparticles on the membrane surface and possible migration of nanoparticles to

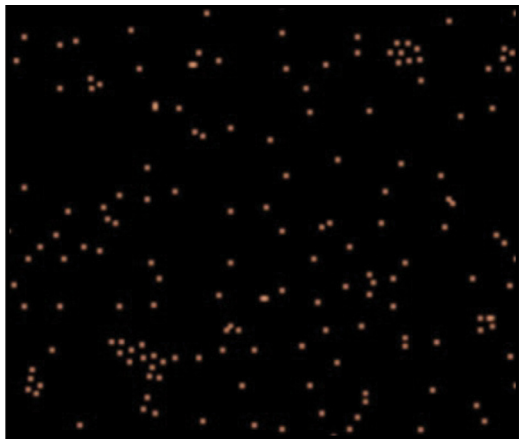

Fig. 7. EDX mapping of Co related to composite nanoparticles in the membrane body: investigation the dispersion of nanoparticles in membrane matrix.

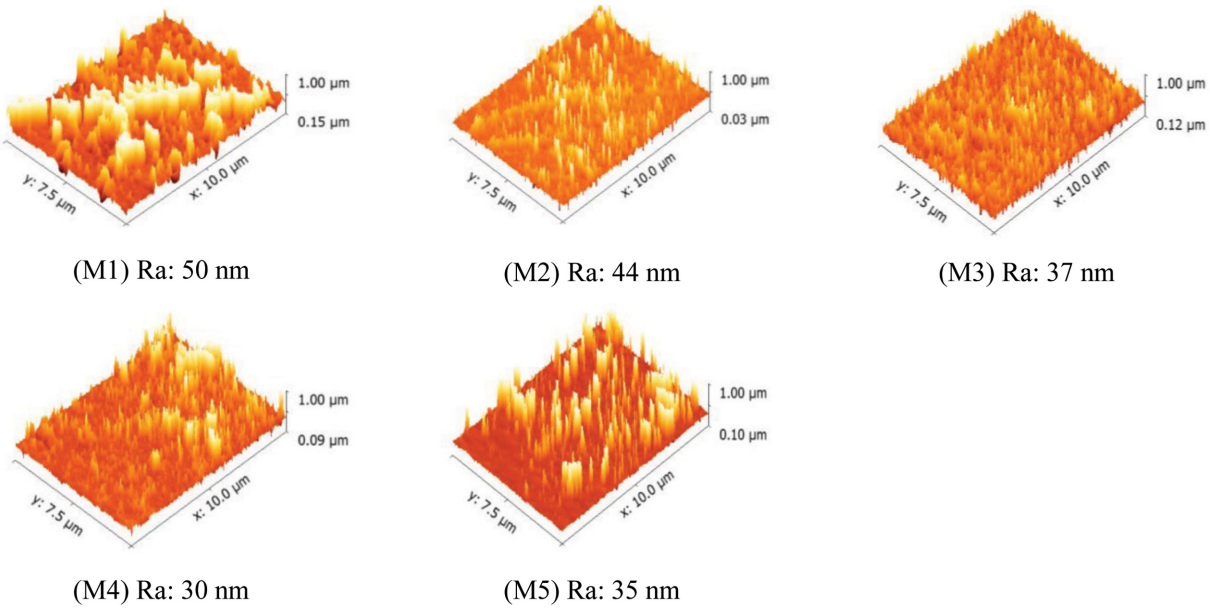

Fig. 8. 3D surface images for all prepared membranes: pristine membrane and mixed matrix membranes.

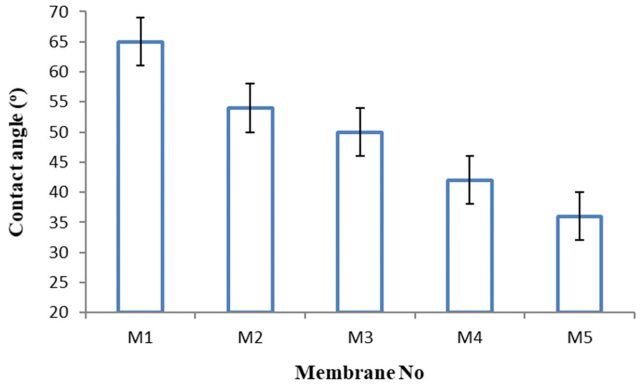

Fig. 9. The water contact angle of fabricated membranes.

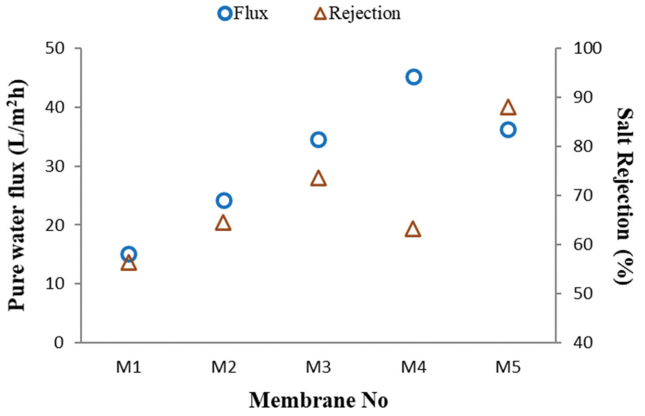

Fig. 10. The effect of nanoparticle concentration on pure water flux and salt rejection.

the membrane surface during the phase inversion process would provide a smoother surface for the blended membranes. Some increase of roughness for M5 at higher nanoparticle loading ratios may be due to possible agglomeration of nanoparticles at its high concentration. Moreover, increase of casting solution viscosity at high additive ratios would decrease the exchange rate between solvent and non-solvent during the formation process, which enhances the possibility of nanoparticle accumulation. The increment of membrane roughness can lead to a suitable surface for bio-fouling [10,42].

2-2. Membrane Surface Hydrophilicity

The surface hydrophilicity of prepared membranes was investigated by contact angle measurement. The contact angle results are shown in Fig. 9. Obtained results show that all modified membranes have lower contact angle compared to virgin PES membrane. The contact angle was reduced from 65° for pure PES membrane to 36° for the blended membranes. Introducing composite nanoparticles into membrane matrix provides more hydrophilic surface for them. This is because of decrease in membrane surface roughness that would enhance the surface hydrophilicity via creating hydrogen bonding between water molecules and nanoparticles on the membrane surface. Also, amino and hydroxyl groups of chitosan in the synthesized Cs-($CoFe_2O_4$/CuO) composite nanoparticles would enhance the membrane hydrophilicity.

2-3. Membrane Filtration Performance

Fig. 10 shows the change of PWF and salt rejection for the prepared membranes by introducing composite nanoparticles into the PES matrix. The PWF was increased from 15.1 (L/m^{2}h) for pristine membrane to 45.2 (L/m^{2}h) for M4 with 0.5 wt% of nanoparticles. The membrane morphology and surface hydrophilicity directly affect filtration performance. The improvement of membrane surface hydrophilicity is a desirable property that would decrease the interfacial energy between water molecules and membrane surface, which promotes the water flux through the membrane [13,17]. Also, as shown in Fig. 11, the increase of membrane porosity makes facile the water molecule transport through the membrane, which enhances the PWF. Decrease of PWF for M5

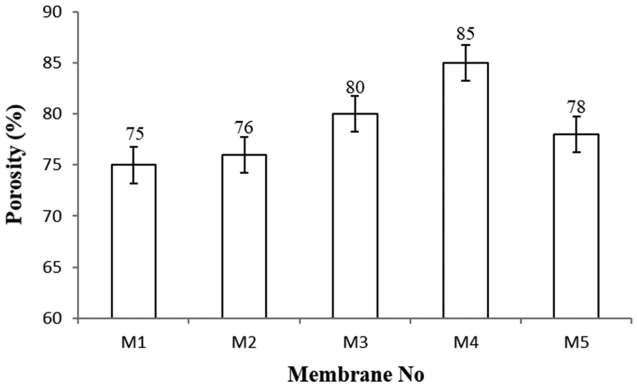

Fig. 11. The overall porosity for fabricated membranes.

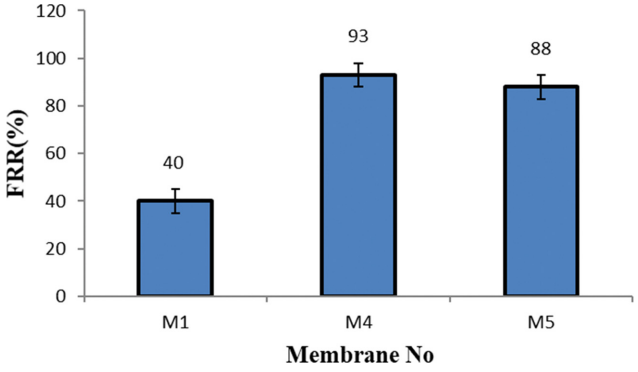

Fig. 13. The flux recovery ratio (FRR%) of neat membrane (M1) and modified membranes (M4, M5).

with 1.0 wt% composite nanoparticles can be explained by membrane pore blocking, nanoparticle accumulation and creating tighter surface for M5 at high additive concentration [47], which reduces the PWF. Besides, decrease of membrane porosity at 1.0 wt% composite nanoparticles decreases the PWF. All blended membranes have higher porosity than unmodified membrane and that is due to increase of exchange rate between solvent and nonsolvent during the phase inversion process, as discussed earlier.

The salt rejection was enhanced obviously from 56.5% for the pristine membrane to 88% for M5 with 1.0 wt% synthesized composite nanoparticles. This is due to the Donnan exclusion effect by amine and hydroxyl groups of composite nanoparticles that repulses the negative ions. Also, the superior adsorption property of composite nanoparticles creates more active sites for ion adsorption. In addition, the possible pore blockage by the nanoparticles limits the salt transport through the membrane, which improves the salt rejection. The increase of membrane surface hydrophilicity by incorporating of composite nanoparticles also reduces the concentration polarization and that improves salt rejection [48]. However, slight decrease of salt rejection for M4 may be because of the highest flux for this sample that makes possible the salt percolation through the membrane.

2-4. Fouling Experiments

Fig. 12 illustrates the change of flux with time for the fabricated membranes during 1 h. The PWF for fresh membranes ($J_{w,1}$), powder milk solution flux (J_p) and the PWF for the washed membranes ($J_{w,2}$) is shown in Fig. 12. Also, Fig. 13 exhibits the flux recovery ratio (FRR%) for the prepared membranes. As seen, M4 with 0.5 wt% synthesized composite nanoparticles has the highest FRR. The hydrophilic property and surface morphology of membrane are two main factors for improvement of antifouling activity of membranes. Increase of membrane surface hydrophilicity decreases the hydrophobic interaction between molecules of foulant and membrane surface by formation of a thin layer of water on its surface. Also, a smoother surface for the membranes reduces the pollutant adsorption on their surface [43,46]. All blended membranes containing Cs-($CoFe_2O_4$/CuO) nanoparticle showed higher fouling resistance than pristine membrane, which is assigned to the more hydrophilic surface and smoother surface for the nanocomposite membranes compared to pristine membrane. Moreover, some decline of FRR% for M5 at high additive concentration may be attributed to possible agglomeration of nanoparticles, which would decrease the effective surface area of nanoparticles. Besides, some increase of surface roughness for M5 decreases its anti-fouling property.

Three parameters, including reversible fouling (R_r), which can be eliminated with hydraulic cleaning, irreversible fouling (R_{ir}) which cannot be eliminated only with hydraulic cleaning, and total fouling (R_t) which is related to total flux loss [40,49], were applied to

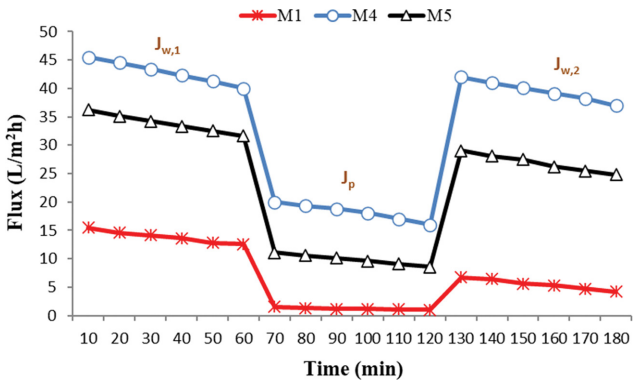

Fig. 12. Change of flux with time for the fabricated membranes during 1 h: neat membrane (M1) and modified membranes with 0.5 wt% (M4) and 1.0 wt% (M5) composite nanoparticles.

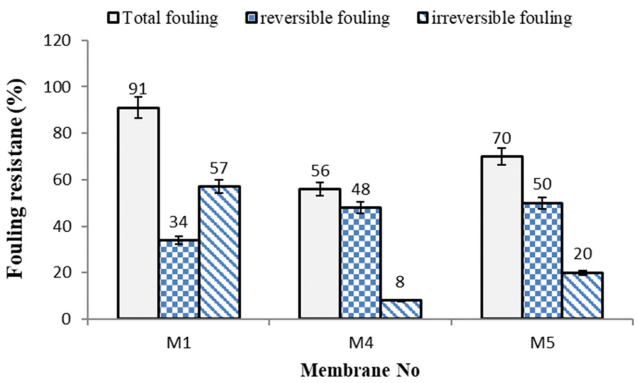

Fig. 14. The fouling parameters for the neat membrane (M1) and the modified membranes (M4, M5).

characterize the fouling resistance of prepared membranes. The results for R_t, R_r and R_{ir} are shown in Fig. 14. The lower value of R_t represents the better fouling resistance, while higher FRR% shows the better antifouling property for the membranes. The pure PES membrane had the highest total fouling ratio (91%) and irreversible fouling (57%) due to lower hydrophilicity and charge of surface for this sample [60]. The highest reversible fouling (50%) that can be removed easily with pure water cleaning was obtained for M5 at 1 wt% of composite nanoparticles. The rougher surface for the membrane leads to increase of foulant adsorption that causes pore blockage. As seen, incorporation of composite nanoparticles into PES matrix reduced the amount of irreversible fouling significantly due to highly hydrophilic property of synthesized nanoparticles. Formation of a water layer as a barrier would decrease the interaction of foulants with membrane surface [18,20]. The results revealed that introducing Cs-($CoFe_2O_4$/CuO) composite nanoparticles into membrane matrix enhances the antifouling property of NF-membranes.

CONCLUSION

Cs-($CoFe_2O_4$/CuO) composite nanoparticles were prepared by chemical precipitation technique and then utilized for the modification of PES-based NF membranes. The effect of Cs-($CoFe_2O_4$/CuO) concentration in the membrane matrix on the physico-chemical properties, separation performance and fouling resistance of them was studied. The XRD, SEM and FTIR results decisively showed formation of Cs-($CoFe_2O_4$/CuO) composite nanoparticles. The SEM images of fabricated membranes also showed more porous with larger voids for the blended membranes compared to pristine membrane. A smoother surface and higher surface hydrophilicity were obtained for the modified membranes than pure PES membrane. The pure water flux of all modified membranes was enhanced significantly compared to pure PES membrane, and the highest pure water flux (45.2 L/m^2h) was obtained for M4 with 0.5 wt% of Cs-($CoFe_2O_4$/CuO) composite nanoparticles. The Na_2SO_4 rejection also improved from 56.5% for the neat membrane to 88% for M5 with 1.0 wt% synthesized nanoparticles. The modified membranes showed significant antifouling resistance. The FRR% measured 93% for M4 with 0.5 wt% composite nanoparticles, while it was 40% for pure PES membrane.

ACKNOWLEDGEMENT

The authors gratefully acknowledge Arak University for the financial support during this research. Farhad Zareei is also thankful to Mr. Ali Ahmadi from Arak University for all useful help and discussions during the preparation of composite nanoparticles.

REFERENCES

1. X. Li, Y. Zhang and X. Fu, *Sep. Purif, Technol.*, **37**, 187 (2004).
2. G. Arthanareeswaran, P. Thanikaivelan, K. Srinivasn, D. Mohan and M. Rajendran, *Eur. Polym. J.*, **40**, 2153 (2004).
3. Z. Kiamehr, B. Farokhi and S. M. Hosseini, *Korean J. Chem. Eng.*, **38**, 114 (2021).
4. Q. Shi, Y. Su, S. Zhu, C. Li, Y. Zhao and Z. Jiang, *J. Membr. Sci.*, **303**, 204 (2007).
5. H. Mo, K. G. Tay and H. Y. Ng, *J. Membr. Sci.*, **315**, 28 (2008).
6. C. Jönsson and A.-S. Jönsson, *J. Membr. Sci.*, **108**, 79 (1995).
7. H. Shon, S. Vigneswaran, I. S. Kim, J. Cho and H. Ngo, *J. Membr. Sci.*, **234**, 111 (2004).
8. C. J. Lin, S. Shirazi, P. Rao and S. Agarwal, *Water Res.*, **40**, 806 (2006).
9. H. Ma, L. F. Hakim, C. N. Bowman and R. H. Davis, *J. Membr. Sci.*, **189**, 255 (2001).
10. D. Rana and T. Matsuura, *Chem. Rev.*, **110**, 2448 (2010).
11. M. T. R. Committee, *Recent advances and research need in membrane fouling*, in AWWA, 79 (2005).
12. J. B. Li, J. W. Zhu and M. S. Zheng, *J. Appl. Polym. Sci.*, **103**, 3623 (2007).
13. J. F. Li, Z. L. Xu, H. Yang, L. Y. Yu and M. Liu, *Appl. Surf. Sci.*, **255**, 4725 (2009).
14. J. Kim and B. Van der Bruggen, *Environ. Pollut.*, **158**, 2335 (2010).
15. S. Ansari, A. R. Moghadassi and S. M. Hosseini, *Korean J. Chem. Eng.*, **37**, 2011 (2020).
16. S. Bandehali, F. Parvizian, A. R. Moghadassi and S. M. Hosseini, in *Nanomaterials for the detection and removal of wastewater pollutants*, B. Bonelli, F. S. Freyria, I. Rossetti, R. Sethi, Elsevier, Amsterdam, Netherlands (2020).
17. S. Bandehali, A. R. Moghadassi, F. Parvizian, J. N. Shen and S. M. Hosseini, *Korean J. Chem. Eng.*, **37**, 263 (2020).
18. S. Bandehali, F. Parvizian, A. R. Moghadassi, J. N. Shen and S. M. Hosseini, *Korean J. Chem. Eng.*, **37**, 1552 (2020).
19. A. Rahimpour, S. Madaeni, A. Taheri and Y. Mansourpanah, *J. Membr. Sci.*, **313**, 158 (2008).
20. S. M. Hosseini, F. Karami, S. Koudzari Farahani, S. Bandehali, J. N. Shen, E. Bagheripour and A. Seidypoor, *Korean J. Chem. Eng.*, **37**, 866 (2020).
21. J. S. Taurozzi, H. Arul, V. Z. Bosak, A. F. Burban, T. C. Voice, M. L. Bruening and V. V. Tarabara, *J. Membr. Sci.*, **325**, 58 (2008).
22. H. Zangeneh, A. A. Zinatizadeh, S. Zinadini, M. Feyzi and D. W. Bahnemann, *Sep. Purif. Technol.*, **209**, 764 (2019).
23. G. Zhang, J. Qu, H. Liu, A. T. Cooper and R. Wu, *Chemosphere*, **68**, 1058 (2007).
24. L. Shao, Z. Ren, G. Zhang and L. Chen, *Mater. Chem. Phys.*, **135**, 16 (2012).
25. E. Salehi, P. Daraei and A. A. Shamsabadi, *Carbohydr. Polym.*, **152**, 419 (2016).
26. M. N. R. Kumar, *React. Funct. Polym.*, **46**, 1 (2000).
27. M. Rinaudo, *Prog. Polym. Sci.*, **31**, 603 (2006).
28. F. Fu and Q. Wang, *J. Environ. Manage.*, **92**, 407 (2011).
29. B. Krajewska, *Sep. Purif. Technol.*, **41**, 305 (2005).
30. W. W. Ngah, L. Teong and M. Hanafiah, *Carbohydr. Polym.*, **83**, 1446 (2011).
31. P. Daraei, S. S. Madaeni, N. Ghaemi, M. A. Khadivi, B. Astinchap and R. Moradian, *J. Membr. Sci.*, **444**, 184 (2013).
32. Z. Wang, Z. Wang, S. Lin, H. Jin, S. Gao, Y. Zhu and J. Jin, *Nat. Commun.*, **9**, 2004 (2018).
33. E. Bagheripour, A. Moghadassi, S. Hosseini, B. Van der Bruggen and F. Parvizian, *J. Ind. Eng. Chem.*, **62**, 311 (2018).
34. E. Bagheripour, A. Moghadassi, S. Hosseini, M. Ray, F. Parvizian

and B. Van der Bruggen, *Chem. Eng. Res. Des.*, **132**, 812 (2018).
35. L. Eckertova, *Physics of thin films*, 2nd Ed., Plenum Press, Berlin, Springer (1986).
36. V. Vatanpour, S. S. Madaeni, R. Moradian, S. Zinadini and B. J. Astinchap, *Sep. Purif. Technol.*, **90**, 69 (2012).
37. S. M. Hosseini, M. Afshari, A. R. Fazlali, S. Koudzari Farahani, S. Bandehali, B. Van der Bruggen and E. Bagheripour, *Chem. Eng. Res. Des.*, **147**, 390 (2019).
38. S. Bandehali, F. Parvizian, A. R. Moghadassi and S. M. Hosseini, *J. Polym. Res.*, **26**, 211 (2019).
39. S. Bandehali, A. Moghadassi, F. Parvizian and S. Hosseini, *Korean J. Chem. Eng.*, **36**, 1657 (2019).
40. F. Zareei and S. M. Hosseini, *Sep. Purif. Technol.*, **226**, 48 (2019).
41. M. Ebrahimi, B. Van der Bruggen, S. M. Hosseini, M. Askari and M. Nemati, *IONICS*, **25**, 1199 (2019).
42. V. Vatanpour, S. S. Madaeni, L. Rajabi, S. Zinadini and A. A. Derakhshan, *J. Membr. Sci.*, **401**, 132 (2012).
43. N. Ghaemi, S. S. Madaeni, A. Alizadeh, P. Daraei, M. M. S. Badieh, M. Falsafi and V. Vatanpour, *Sep. Purif. Technol.*, **96**, 214 (2012).
44. J. Yin, G. Zhu and B. Deng, *Desalination*, **379**, 93 (2016).
45. S. Xia, L. Yao, Y. Zhao, N. Li and Y. Zheng, *Chem. Eng. J.*, **280**, 720 (2015).
46. P. Daraei, S. S. Madaeni, N. Ghaemi, E. Salehi, M. A. Khadivi, R. Moradian and B. Astinchap, *J. Membr. Sci.*, **415**, 250 (2012).
47. S. S. Madaeni, S. Zinadini and V. Vatanpour, *Sep. Purif. Technol.*, **111**, 98 (2013).
48. C. Zhao, X. Xu, J. Chen and F. Yang, *J. Environ. Chem. Eng.*, **1,** 349 (2013).
49. H. Yu, Y. Cao, G. Kang, J. Liu, M. Li and Q. Yuan, *J. Membr. Sci.*, **342**, 6 (2009).